Atherosclerosis 283 (2019) 127–136

Contents lists available at ScienceDirect

Atherosclerosis

journal homepage: www.elsevier.com/locate/atherosclerosis

Dual roles of heparanase in human carotid plaque calcification

Silvia Aldi[a,1], Linnéa Eriksson[a,1], Malin Kronqvist[a], Mariette Lengquist[a], Marie Löfling[a], Lasse Folkersen[b], Ljubica P. Matic[a], Lars Maegdefessel[c,d], Karl-Henrik Grinnemo[a], Jin-Ping Li[e], C. Österholm[a,*,1], Ulf Hedin[a,1]

[a] Department of Molecular Medicine and Surgery, Bioclinicum J8:20, Karolinska Institutet, 171 64, Solna, Sweden
[b] Center for Biological Sequence Analysis, Technical University of Denmark, Copenhagen, Denmark
[c] Department of Medicine Solna, L8:03, Karolinska Institutet, 171 76, Stockholm, Sweden
[d] Department of Vascular Surgery, Technical University Munich, 80333, Munich, Germany
[e] Department of Medical Biochemistry and Microbiology, SciLifeLab Uppsala, The Biomedical Center, Husargatan 3, Uppsala University, 752 37, Uppsala, Sweden

HIGHLIGHTS

- Heparanase mRNA levels correlate with osteolytic genes in atherosclerotic lesions.
- Heparanase is expressed by osteoclast-like cells surrounding calcified regions.
- Heparanase promotes calcification of human vascular smooth muscle cells *in vitro*.
- Our findings suggest a bimodal context-dependent role for heparanase in calcification.

ARTICLE INFO

Keywords:
Atherosclerosis
Calcification
Heparanase
Bone remodeling
Heparan sulfate proteoglycans

ABSTRACT

Background and aims: Calcification is a hallmark of advanced atherosclerosis and an active process akin to bone remodeling. Heparanase (HPSE) is an endo-β-glucuronidase, which cleaves glycosaminoglycan chains of heparan sulfate proteoglycans. The role of HPSE is controversial in osteogenesis and bone remodeling while it is unexplored in vascular calcification. Previously, we reported upregulation of HPSE in human carotid endarterectomies from symptomatic patients and showed correlation of HPSE expression with markers of inflammation and increased thrombogenicity. The present aim is to investigate HPSE expression in relation to genes associated with osteogenesis and osteolysis and the effect of elevated HPSE expression on calcification and osteolysis *in vitro*.

Methods: Transcriptomic and immunohistochemical analyses were performed using the Biobank of Karolinska Endarterectomies (BiKE). *In vitro* calcification and osteolysis were analysed in human carotid smooth muscle cells overexpressing HPSE and bone marrow-derived osteoclasts from *HPSE*-transgenic mice respectively.

Results: HPSE expression correlated primarily with genes coupled to osteoclast differentiation and function in human carotid atheromas. HPSE was expressed in osteoclast-like cells in atherosclerotic lesions, and *HPSE*-transgenic bone marrow-derived osteoclasts displayed a higher osteolytic activity compared to wild-type cells. Contrarily, human carotid SMCs with an elevated HPSE expression demonstrated markedly increased mineralization upon osteogenic differentiation.

Conclusions: We suggest that HPSE may have dual functions in vascular calcification, depending on the stage of the disease and presence of inflammatory cells. While HPSE plausibly enhances mineralization and osteogenic differentiation of vascular smooth muscle cells, it is associated with inflammation-induced osteoclast differentiation and activity in advanced atherosclerotic plaques.

* Corresponding author. Department of Molecular Medicine and Surgery, Experimental Cardiothoracic Surgery (ECTS), Bioclinicum J8:20, SE-171 64, Solna, Sweden.
E-mail address: cecilia.osterholm.corbascio@ki.se (C. Österholm).
[1] These authors contributed equally to this work.

https://doi.org/10.1016/j.atherosclerosis.2018.12.027
Received 6 September 2018; Received in revised form 30 November 2018; Accepted 20 December 2018
Available online 05 January 2019
0021-9150/

1. Introduction

Ischemic stroke as a consequence of carotid atherosclerotic plaque instability and rupture is an important cause of death and disability worldwide. Destabilizing processes include neovascularization and infiltration of inflammatory cells that release matrix-degrading enzymes, resulting in fibrous cap thinning. How calcification contributes to plaque vulnerability is unclear, and micro- and macro intimal calcification have been suggested to influence plaque stability differently [1–4]. While originally believed to be a result of passive precipitation of calcium phosphate in the vessel wall, vascular calcification is now regarded as an active process, which shares features with bone remodeling and is mediated by chondrocyte/osteoblast- and osteoclast-like cells transformed from cells of mesenchymal or myeloid origin [5–7].

Heparan sulfate proteoglycans (HSPGs) are composed of long, linear and variably sulfated glycosaminoglycans (GAGs) that are covalently attached to specific core proteins. Depending on the core protein identity, HSPGs are located at the cell surface or in the extracellular matrix (ECM) where they exhibit different functions accordingly [8–10]. For normal bone development and growth and also stem cell commitment towards the osteogenic lineage, HSPGs are vital co-receptors for relevant growth factors such as FGF-2, BMPs and Wnt [11–14]. Heparanase (HPSE) is an endo-β-glucuronidase, which cleaves glycosaminoglycan chains of HSPGs [15]. As HSPGs are important structural entities of the ECM and also sequester a wide range of protein ligands, their degradation by HPSE results in disrupted matrix integrity but may also lead to release of the stored growth factors. HPSE is recognized for its pro-metastatic properties and increased expression levels correlate with a poor outcome in a variety of malignancies [16,17]. In contrast to the well-characterized functions of HPSE in neoplasia, the understanding of its role in the progression and destabilization of atherosclerotic plaques is still limited [18]. We have previously reported on the upregulation of HPSE in human carotid endarterectomies from symptomatic patients and its high levels of correlation with markers of inflammation and increased thrombogenicity [19]. The role of HPSE in vascular calcification is however not known and the few existing reports about HPSE and calcification in general, are conflicting. In a study by Kram et al. [20] transgenic mice overexpressing human HPSE (*hpa*-tg) [21] displayed increased trabecular bone mass and also increased rates of bone formation. A pro-osteogenic function of HPSE was corroborated *in vitro*, where exogenously added HPSE induced osteogenic differentiation of cultured MC3T3 E1 osteoblastic cells. In another study by Manton et al. long-term treatment of human mesenchymal stem cells with heparan sulfate (HS)- and chondroitin sulfate (CS)-degrading enzymes increased osteogenic differentiation, which was ascribed to altered BMP and Wnt activity secondary to disrupted cell surface proteoglycan expression [22]. On the contrary, in multiple myeloma increased HPSE expression levels in tumor cells has been associated with rapid progression of the disease and also with accelerated osteolysis via upregulation of RANKL and stimulation of osteoclastogenesis [23]. Additionally, in the same context, HPSE has been demonstrated to inhibit osteoblastogenesis and bone formation, implicating a significant role for this protein in pathologic bone remodelling [24].

In view of the importance of HSPGs for bone development and the previously reported contradicting roles of HPSE in bone remodelling, the present study aimed to investigate the function(s) of HPSE in vascular calcification. We utilized the BiKE biobank of human carotid atherosclerotic endarterectomy samples in order to expound HPSE expression in relation to genes tightly associated with osteogenesis and osteolysis. Furthermore, we investigated the effect of HPSE expression on calcification and osteolysis *in vitro*.

2. Materials and methods

2.1. Gene expression analysis on human carotid tissue

Human carotid endarterectomy samples from 127 patients undergoing surgery for asymptomatic or symptomatic carotid stenosis were part of the Biobank of Karolinska Endarterectomies (BiKE). Symptoms include minor stroke, transient ischemic attack (TIA) and amaurosis fugax. All samples were collected with consent from patients, organ donors or organ donors' guardians. The regional Ethics Board of Northern Stockholm approved the study. RNA extracted from endarterectomy specimens was analysed by Affymetrix HG-U133 plus 2.0 Genechip arrays. Robust multi-array average (RMA) normalization was performed and processed gene expression data was returned in a $\log_2$-scale. The microarray dataset is available from Gene Expression Omnibus (GSE21545). Regarding multiple probe sets existing for the gene *RUNX2*, re-alignment of these was performed using the GeneRegionScan package (version 1.26.0) from the R/Bioconductor repository [25]. Briefly, the specific nucleotide sequences of each *RUNX2* probe set were extracted and re-aligned to both the mRNA and DNA sequence of the latest human genome build (hg38). This allowed determining both the genome-wide uniqueness of each probe and the precise matching location in the *RUNX2* gene.

2.2. Immunohistochemistry

All immunohistochemistry reagents were from Biocare Medical (Concord, CA). Isotype rabbit and mouse IgG were used as negative controls. In brief, 5 μm sections from zink-formaldehyde fixed and paraffin embedded tissue were de-paraffinized in Tissue Clear and rehydrated in a 99-96-70% ethanol series. For antigen retrieval, slides were subjected to high-pressure boiling in DIVA buffer. After blocking with Background Sniper solution, primary antibodies diluted in Da Vinci Green solution were applied to the sections and incubated at room temperature for 1 h. The primary antibodies were; rabbit polyclonal antibody against HPSE (LifeSpan Biosciences Inc., Seattle, WA) and mouse monoclonal antibodies against TRAP (clone 9C5, LifeSpan Biosciences Inc.), osteocalcin (clone 190125, R&D systems, Abingdon, UK), αSMA (clone M0851, DAKO, Glostrup, Denmark), CD163 (clone 10D6, Abcam, Cambridge, UK) and CD68 (clone 514H12, Novocastra, Newcastle upon Tyne, UK). A probe-polymer system containing alkaline phosphatase was applied to the sections, with subsequent detection using Vulcan Fast Red. The sections were counterstained with Hematoxylin QS (Vector Laboratories, Peterborough, UK). For visualization of precipitated calcium, consecutive sections were stained with Alizarin Red (AZR) from Sigma-Aldrich (St Louis, MO).

2.3. Osteoclast activity assay

Bone marrow was isolated as described previously [26]. Bone marrow cells were counted and plated in α-MEM (Thermofisher Scientific) supplemented with 10 U/ml penicillin/streptomycin, 10% FBS and 30 ng/ml of murine M-CSF (Peprotech EC Ltd, London, UK) at a density of 2–3 x 10^6 cells/ml. After 24h the non-adherent cell fraction was recovered and used for further differentiation towards osteoclasts. For immunofluorescence cells were plated in an IBIDI® chamber (IBIDI, Martinsried, Germany). For quantification of osteolytic activity, 80 000 cells/well were seeded on a synthetic bone surface (Corning Osteo Assay Surface®) provided in 96-well format (Corning). In both instances, the surfaces were pre-coated with human vitronectin (20 μg/ml, Peprotech). After three days, murine RANKL (100 ng/ml, Peprotech) was added for another three days until multi-nucleated cells had formed. Cells in the IBIDI chambers were washed with PBS and fixed in 4% paraformaldehyde and thereafter stained with phalloidin (DyLight™ 554 Phalloidin, Life Technologies) and counterstained with DAPI. For quantitative assessment of resorption pits, the Corning OsteoAssay

surface wells were first stained with DAPI and photographed for documentation of cell density. The wells were subsequently incubated with 10% bleach for 20 min and thereafter thoroughly rinsed with deionized water. After drying, resorption pits where the underlying plastic material was clearly visible, were identified with phase-contrast microscopy, photographed and counted.

2.4. Lentivirus-mediated overexpression of HPSE

Human smooth muscle cells isolated from the carotid artery (HCtASMCs) were purchased from Cell Applications Inc. (San Diego, CA). The cells were maintained in complete smooth muscle cell growth medium (Cell Applications Inc.) and used for transduction and osteogenic differentiation at passages 5–10. Human embryonic kidney cells 293T (ATCC, Manassas, VA) were cultured in DMEM containing Glutamax and supplemented with 10% fetal bovine serum and 10U/ml penicillin/streptomycin (Thermofisher Scientific, Waltham, MA, USA). The pLenti6/V5-DEST (Invitrogen, Carlsbad, CA) vector containing full-length cDNA of the *HPSE1* gene and a blasticidin-resistance selection marker was utilized as transfer plasmid (hpa) for the generation of lentiviral particles. The identical plasmid lacking *HPSE1* cDNA (empty vector, ev) served as a negative control in addition to no transduction (wild-type, wt). Lentiviral particles were harvested from culture supernatants of 293T cells co-transfected with transfer plasmid and the pantropic Virasafe Lentiviral Packaging System (Cell Biolabs Inc., San Diego, CA). HCtASMCs were incubated overnight with the filtered 293T culture supernatants and successfully transduced cells were selected with 2 μg/ml blasticidin (Life Technologies, Carlsbad, CA) for further expansion and functional assays. The initial transduction efficiency was approximately 50% for both the hpa and ev transfer plasmids, which became evident after 2 days of blasticidin treatment, when half of the cells died in both cell cultures. This indicates that HPSE-overexpressing and control cells were infected with comparable numbers of virus particles. The three resulting subgroups of HCtASMCs are hereafter referred to as “hpa”, “ev” and “wt” HCtASMCs, respectively.

2.5. Western blot

Cultured HCtASMCs were harvested and lysed in RIPA buffer (Sigma Aldrich) containing protease inhibitor cocktail (cOmplete ultra tablets mini, EDTA-free, easy pack, Roche Applied Science, Mannheim, Germany) and protein concentrations were determined using the BCA protein assay kit (ThermoFischer Scientific). For wt and ev HCtASMCs, 60 μg of protein were used and for hpa HCtASMCs, 6 μg were used. Samples were separated by SDS-PAGE and subsequently blotted onto PVDF membranes. After blocking and staining with rabbit-anti-human HPSE antibody (LifeSpan Biosciences Inc.) and thereafter HRP-conjugated goat-anti-rabbit antibody, the membrane was incubated in ECL Advance (GE Healthcare) and exposed to film. Subsequently the membrane was stripped using Millipore Re-blot solution and thereafter re-probed with a mouse-anti-human α-tubulin antibody (#3873, Cell Signaling, Leiden, The Netherlands).

2.6. Flow cytometry

Cell suspensions of hpa, ev and wt HCtASMCs were washed and incubated for 30 min at 4 °C with a 1:100 dilution of mouse monoclonal anti-human heparan sulfate antibody (clone F58-10E4, Amsbio, Abingdon, UK) in PBS containing 3% FBS. After 3 washes in PBS (3% FBS), cells were incubated with Alexa Fluor488-conjugated goat-anti-mouse IgM (5 μg/ml)(Thermo Fischer Scientific), washed and analysed on a FACSCalibur (BD Biosciences). Cells stained with secondary antibody alone served as negative control.

2.7. Quantitative real-time RT-PCR

RNA was extracted from cells lysed in Qiazol, using the miRNeasy mini kit (Qiagen, Hilden, Germany). Five hundred ng of RNA were reversely transcribed into cDNA using the High Capacity RNA-to-cDNA kit (Applied Biosystems, Foster City, CA) and 1 μl of the reaction was subsequently used for real-time PCR. The probes for *HPSE* (Hs00935036_m1), *SPP1* (osteopontin) (Hs00959010_m1), *RUNX2* (Hs00231692_m1) and *RPLPO* (Hs99999902_m1, house-keeping gene) were purchased from Applied Biosystems.

2.8. Osteogenic differentiation

HCtASMCs were seeded in 48-well plates at a density of 30 000 cells/well or in 12-well plates at a density of 100 000 cells/well and cultured in SMC growth medium until 80% confluency. For scanning electron microscopy (SEM), the cells were seeded on coverslips in the 12-well plate format. The growth medium was replaced with human StemMACS OsteoDiff Media (Miltenyi Biotec, Germany) supplemented with Mycozap Antibiotics, (Lonza, Switzerland) and the cells were cultured for 4 or 21 days, with or without supplemented unfractionated heparin (10μg/ml or 2.12 IU/ml, Hepalink Pharmaceuticals, Shenzhen, China). This concentration was used based on pilot assays where higher levels negatively affected the viability, primarily of hpa HCtASMCs (data not shown). The differentiation medium was changed twice per week. At the end of each incubation period alkaline phosphatase activity was assessed by using the Sigma*FAST* BCIP/NBT (Sigma-Aldrich) substrate according to the manufacturers' instructions. Cells stained blue were counted manually in a blinded fashion on 5 images taken at 10x magnification from each condition and normalized against total numbers of cell nuclei in corresponding phase contrast images. Mineralization was visualized and photographed in parallel wells after incubation with Alizarin Red solution (Millipore) for 40 min and subsequent rinses with distilled water to remove unbound stain. For SEM cells were fixed by immersion in 2,5% glutaraldehyde in 0.1M PB (pH 7.4). The specimens were briefly rinsed in distilled water and placed in 70% ethanol for 10 min, 95% ethanol for 10 min, absolute ethanol for 15 min at room temperature and in pure acetone for 10 min. Specimens were then dried using a critical point dryer (Balzer, CPD 010, Lichtenstein) using carbon dioxide. After drying, specimens were mounted on an aluminium stub and coated with Platinum (Bal-Tec SCD 005, Lichtenstein).

2.9. Microscopy

Histological sections were photographed using (Nikon OPTIPHOT-2 microscope equipped with digital camera and NIS-Elements software) together with the NIS elements software. Cells undergoing osteogenic or osteoclastic differentiation were captured using an IX81 microscope (Olympus) and the XC10 camera (Olympus Soft Imaging Solutions) and subsequent automated or manual counting of cells/nuclei was facilitated by using the CellSens or ImageJ software, respectively. For SEM, the specimens were analysed in an Ultra 55 field emission scanning electron microscope (Zeiss, Oberkochen, Germany) at 3 kV.

2.10. Statistics

Comparisons between groups of tissue samples in BiKE as well as comparisons between cell culture treatments were performed using a one-way analysis of variance (ANOVA) with Bonferroni post hoc testing (for group numbers ≥ 3) or the Mann-Whitney *U* test (for group numbers = 2). Correlations between expression levels of HPSE and genes of interest were done using Spearman correlation with Bonferroni correction for multiple comparisons. Prism software (Graphpad, San Diego, CA) was used for all statistical analyses and $p < 0.05$ was considered to indicate statistical significance.

Table 1
HPSE gene expression levels correlate with markers of bone resorption in human carotid atherosclerotic lesions.

Spearman correlation analysis with Bonferroni correction was performed on microarray data from human carotid endarterectomies to identify correlations between mRNA levels of HPSE and genes mainly associated with osteogenesis and osteolysis, respectively. Runx2 (I) represents the 3′ probe set 232231_at, targeting the 5′UTR and Runx2 (II) is representative of the remaining probe sets.

Gene	Protein	Spearman r	*p*-value
RUNX2	Runx2 (I)	**−0.20**	n.s.
RUNX2	Runx2 (II)	**0.58**	< 0.001
BGLAP	Osteocalcin	**−0.12**	n.s.
BMP2	BMP2	**−0.07**	n.s.
TNFSF11	RANKL	**0.13**	n.s.
TNFRSF11B	OPG	**−0.23**	n.s.
SOX9	Sox9	**0.08**	n.s.
MSX2	Msx2	**−0.08**	n.s.
SPARC	SPARC	**−0.28**	< 0.05
ALPL	ALP	**−0.14**	n.s.
IBSP	Bone sialoprotein	**0.29**	< 0.05
MGP	Matrix Gla Protein	**−0.44**	< 0.01
SPP1	Osteopontin	**0.58**	< 0.01
ACP5	TRAP	**0.73**	< 0.01
TNFRSF11A	RANK	**0.52**	< 0.01
OSCAR	OSCAR	**0.76**	< 0.01

P < 0.05 was considered to indicate statistical significance.

3. Results

3.1. HPSE mRNA levels correlate with expression of genes associated with osteoclast differentiation and function in human carotid atherosclerotic lesions

To investigate whether HPSE is primarily associated with formation or degradation of calcified structures within atherosclerotic tissue, *HPSE1* expression levels were correlated to expression of pro-calcific or osteolytic genes (Table 1). Apart from a weak positive correlation with bone sialoprotein (*IBSP*), no correlations could be found between and pro-osteogenic genes, such as *BGLAP*, *SOX9*, *MSX2* and *SPARC*. As for *RUNX2*, which is recognized as a key regulator of osteoblast differentiation and inducer of calcification [27], there was a negative or absent correlation with *HPSE1,* except for one out of the 6 *RUNX2* probe sets on the microarray, targeting the 5'UTR of the gene and which demonstrated a strong positive correlation (r = 0.58) (Supplementary Fig. 1). *HPSE1* mRNA levels showed strong, positive correlation with mediators of osteoclast differentiation/activity and/or inhibitors of mineralization, such as TRAP, RANK and OSCAR. However, as a contrasting result to the clear trends observed, the correlation between Matrix Gla protein (*MGP*) and *HPSE1* was significantly negative (Table 1).

3.2. Expression of calcification-associated genes in carotid atherosclerotic lesions from symptomatic vs asymptomatic patients

In our previous study, an increase in HPSE expression was associated with an unstable plaque phenotype [19]. In order to determine whether this was the case also for genes showing a strong positive correlation with HPSE in the current study, we compared the mRNA expression levels of genes included in the correlation assay, in symptomatic vs asymptomatic patients. The osteoclast-associated genes encoding *TRAP* and *OSCAR* were significantly upregulated in unstable lesions (Table 2). This also corroborates the findings of another of our previous studies, aiming at identifying the dominant signaling pathways and gene networks in BiKE, and where the gene ontology process "positive regulation of bone resorption" was enriched in symptomatic vs asymptomatic patients [4].

Table 2
Increased expression of osteoclast-associated genes in carotid plaques from symptomatic patients.

mRNA expression levels of twelve genes implicated in bone formation or bone resorption were compared in carotid lesions from asymptomatic *vs.* symptomatic patients, using Mann-Whitney *U* Test. Values (log_2) are shown as mean ± SEM.

Gene	Alias	Asymptomatic (n = 40)	Symptomatic (n = 85)	*p*-value
BGLAP	Osteocalcin	5.304 ± 0.068	5.237 ± 0.044	n.s.
RUNX2	RUNX2	3.214 ± 0.041	3.207 ± 0.024	n.s.
BMP2	BMP2	5.234 ± 0.095	5.396 ± 0.071	n.s.
TNFSF11	RANKL	3.104 ± 0.055	3.248 ± 0.047	n.s.
SPP1	Osteopontin	13.09 ± 0.138	13.42 ± 0.040	n.s.
ACP5	TRAP	9.804 ± 0.201	10.31 ± 0.099	< 0.001
TNFRSF11A	RANK	5.043 ± 0.091	5.096 ± 0.058	n.s.
SOX9	SOX9	5.371 ± 0.081	5.443 ± 0.058	n.s.
MSX2	MSX2	4.249 ± 0.050	4.203 ± 0.029	n.s
IBSP	Bone Sialoprotein	6.812 ± 0.137	7.162 ± 0.105	n.s.
TNFRSF11B	Osteoprotegerin	9.390 ± 0.085	9.229 ± 0.074	n.s
OSCAR	OSCAR	5.831 ± 0.146	6.255 ± 0.086	< 0.01

3.3. HPSE co-localizes with TRAP in multi-nucleated cells of monocytic origin but not with osteocalcin-rich calcified regions in human carotid atherosclerotic lesions

In order to determine if the correlations between HPSE and different osteo-associated factors observed at the gene expression level could be corroborated *in situ* by overlapping protein expression patterns, immuno-histochemical stainings were performed on consecutive sections of human carotid atherosclerotic lesions. TRAP-positive multi-nucleated cells were identified adjacent to heavily calcified regions however, they were more abundant in dystrophically calcified regions that were also densely infiltrated with inflammatory cells (Fig. 1A, C and B). HPSE staining was abundant in TRAP-positive osteoclast-like cells (Fig. 1D) generally residing in plaque regions with inflammatory infiltrates. Both CD68- and CD163-positive macrophages were present in these regions, although large, TRAP-positive cells containing a large number of nuclei, tended to be CD68-positive while staining negative for CD163 (Fig. 1E–F). In sub-intimal SMC-rich regions, where the osteoblast marker osteocalcin could be observed within areas of mineralization, HPSE staining was weak or absent (Fig. 2).

3.4. Increased osteolytic activity by osteoclasts derived from murine bone marrow overexpressing HPSE

As HPSE mRNA levels showed strong positive correlations with those of osteoclast markers in the BiKE database and was also expressed by this cell type in histological sections of carotid atherosclerotic lesions, we investigated the effect of increased HPSE expression levels on the osteolytic activity of osteoclasts. We used *hpa*-tg mice, as bone marrow from these animals has previously been demonstrated to degrade HS to an increased extent compared to wt cells [20]. Osteoclasts differentiated from the myeloid fraction from *hpa*-tg displayed a varying but altogether significantly increased number of resorption pits (mean = 98 ± 120) in comparison to osteoclasts from wt mice (mean = 10.7 ± 5.5) (Fig. 3A). The absolute pit numbers where higher, and as the number of monocytic cells adhering to the bone matrix after incubation with M-CSF was consistently smaller for *hpa*-tg cells, the difference increased further when normalizing pit numbers to the total numbers of adhering cells. Although osteoclasts from both wt and *hpa*-tg mice tended to vary with regard to size and morphology (Fig. 3B–C), there was no apparent difference in relation to the size of the pits generated (Fig. 3D–E).

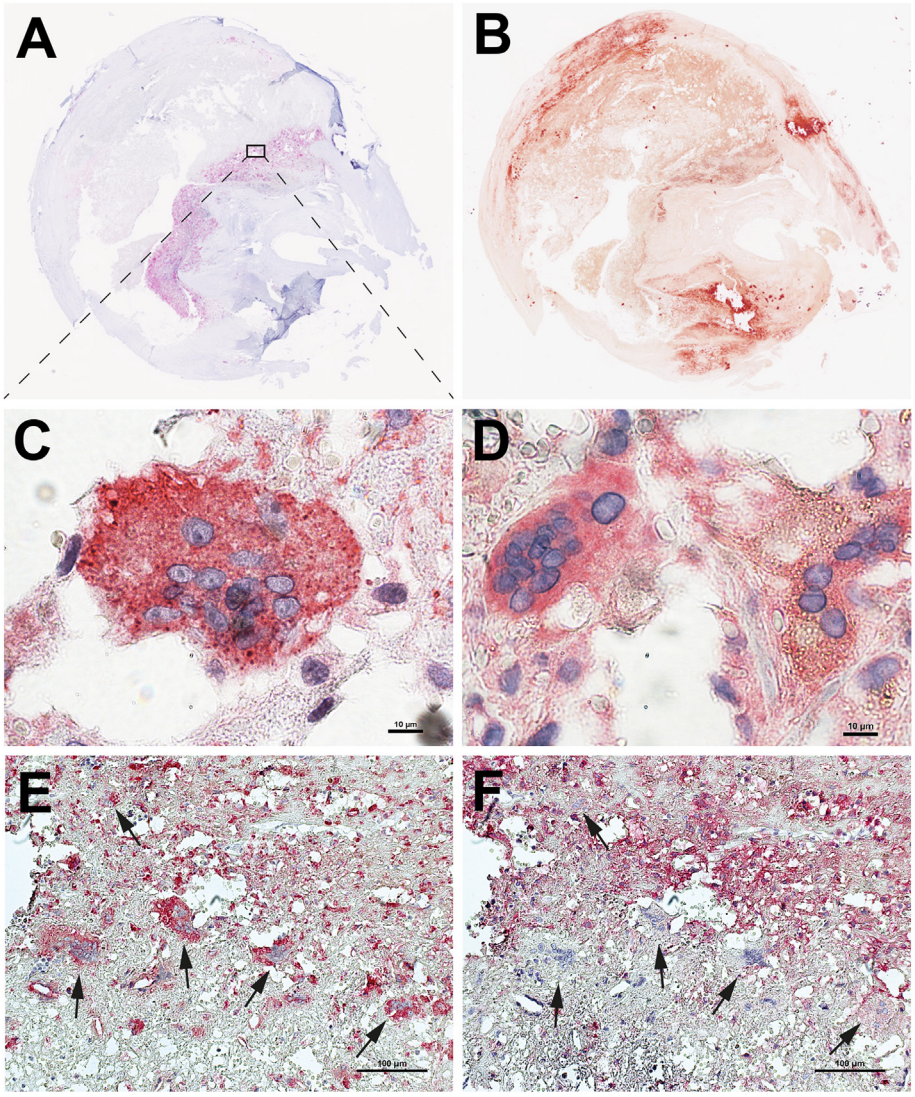

Fig. 1. HPSE is expressed by osteoclast-like cells in human carotid atherosclerosis.
TRAP-positive multinucleated cells stained with red chromogen (A), (C) were frequently distributed in regions of inflammatory infiltrates and dystrophically calcified tissue. Calcification was visualized by Alizarin Red staining of an adjacent section (B). HPSE (red chromogen) was expressed by multi-nucleated osteoclast-like cells, some of which appeared to be actively resorbing calcified structures (golden color) within the plaque (D). Large, multinucleated osteoclast-like cells in the human carotid plaques were generally positive for macrophage marker CD68 (E, red chromogen) and negative for macrophage marker CD163 (F, red chromogen) as shown in consecutive sections containing the same cells. Size bars correspond to 500 µm in (A) and (B), to 10 µm in (C) and (D) and to 100 µm in (E) and (F).

3.5. *Increased osteogenesis in human carotid SMCs overexpressing HPSE*

Although a variety of cell types have been suggested to induce or mediate the calcification process in blood vessels [28,29], vascular SMCs are the most extensively investigated with regard to their phenotypic plasticity and ability to acquire chondrogenic and osteogenic properties *in vitro* as well as *in vivo* [6,30,31]. To assess the effect of increased HPSE expression on osteogenic differentiation of human

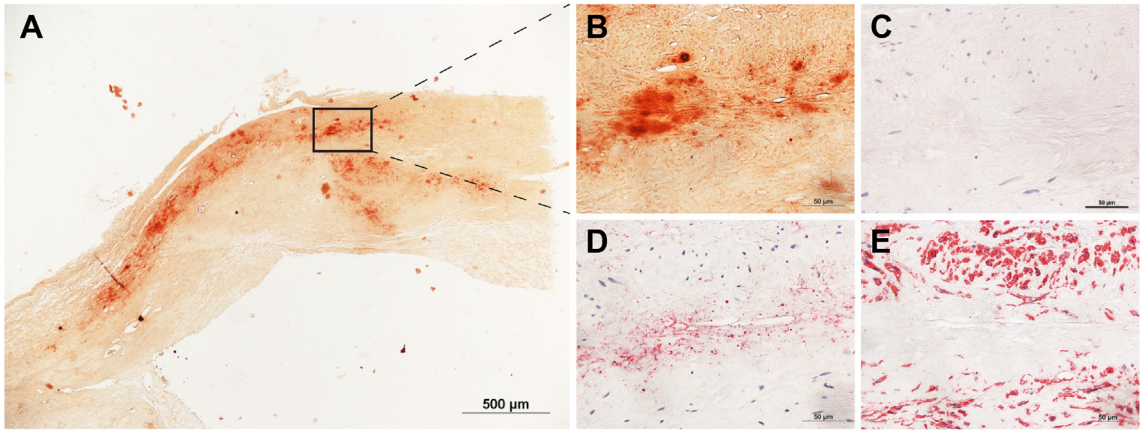

Fig. 2. HPSE expression is absent in calcified regions of carotid atherosclerotic lesions.
Consecutive histological sections of a representative plaque were stained with Alizarin Red (A–B) or antibodies against HPSE (C), osteocalcin (D) and smooth muscle α-actin (E). The close-up image from the plaque sub-region, indicated by the box in A, shows the same area on consecutive sections, in B-E. Positive staining is shown as dark orange (A–B) or red (C–E). Size bars represent 50 µm in (B–E).

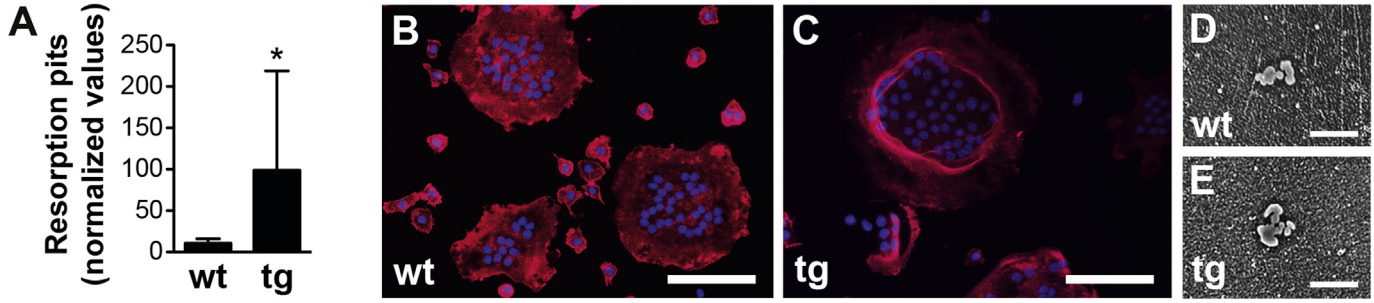

Fig. 3. Increased osteolytic activity in osteoclasts from *hpa-tg* mice.
Non-adherent fractions of bone marrow from wt and hpa-*tg* mice respectively were plated and differentiated with M-CSF and RANKL on vitronectin-coated artificial bone surfaces for 3 + 3 days. Osteoclasts derived from wt and hpa-*tg* bone marrow were stained with DyLight™ 554 Phalloidin (red) and DAPI (blue) (A–B). Representative resorption pits formed by wt and hpa-*tg* osteoclasts after incubation on artificial bone surfaces (C–D). Resorption pits were counted and normalized against numbers of DAPI-stained cell nuclei in (control) wells with cells incubated with M-CSF, without addition of RANKL (E). Each cell type was assessed in triplicate (n = 4) for each condition and experiments were repeated twice. *$p < 0.05$. Size bars represent 100 μm in (B) and (C), and 30 μm in (D) and (E).

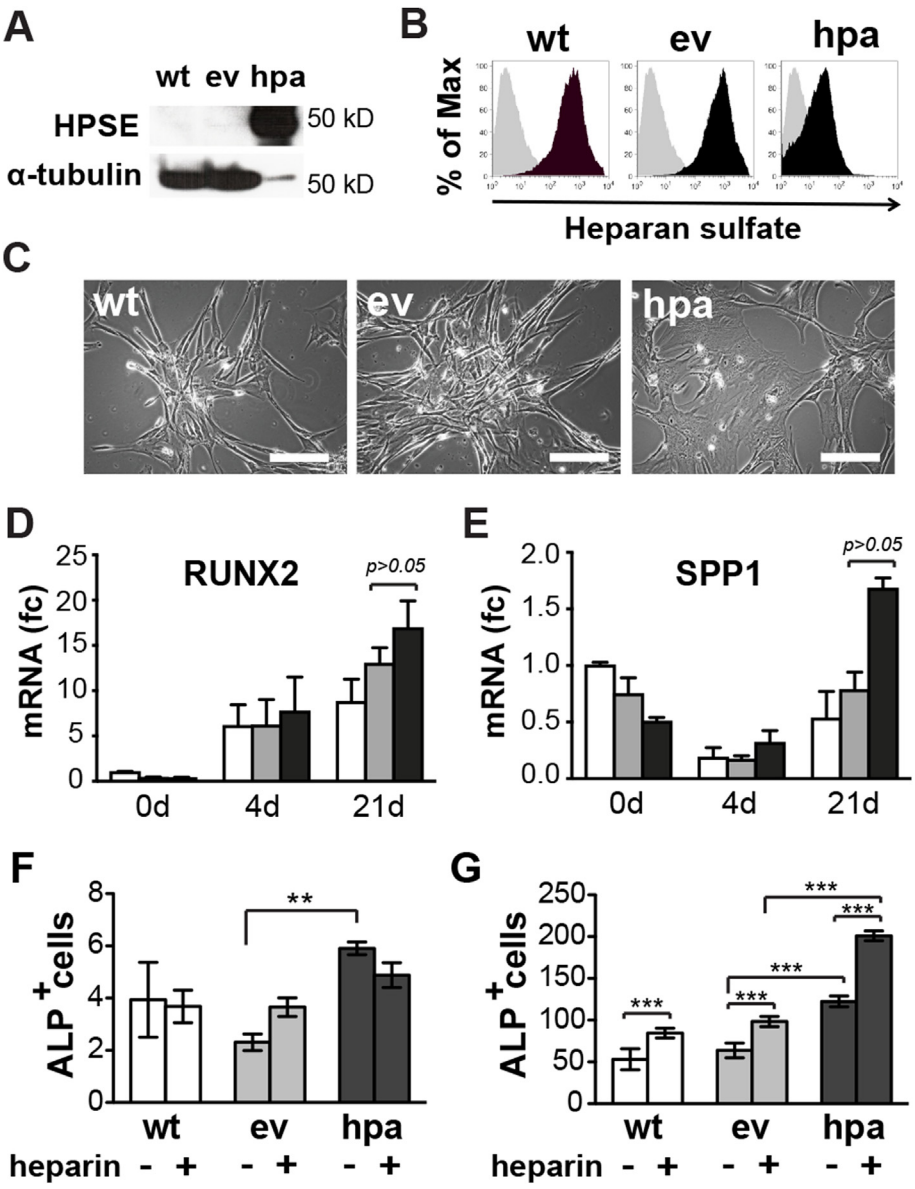

Fig. 4. Increased HPSE expression enhances osteogenic differentiation of human carotid SMCs *in vitro*.
HPSE overexpression in HCtASMCs was assessed after transduction with lentiviral vectors (wt = wildtype, ev = empty vector, hpa = vector encoding full-length human *HPSE1* cDNA). (A) HPSE transgene expression at the protein level, shown with western blot. For wt and ev HCtASMCs, 60 μg of protein were used and for hpa HCtASMCs, 6 μg were used (B) FACS histograms depicting cell surface heparan sulfate (HS) expression after staining with anti-HS antibody 10E4. (C) Morphology of wt, ev and hpa HCtSMCs. (D–E) Gene expression levels of *RUNX2* and *SPP1* (osteopontin) were analysed at 4 days and 21 days of incubation with osteogenic differentiation medium; white bars = wt, grey bars = ev, black bars = hpa. Each cell type was plated in duplicate for each condition and experiments were repeated twice. Normalized numbers of wt (white bars), ev (grey bars) and hpa (black bars) HCtASMCs positive for alkaline phosphatase activity are shown at 4 days (F) and 21 days (G) of osteogenic differentiation with or without the addition of heparin. Each cell type was assessed in triplicate (n = 3) for each condition and experiments were repeated 3 times. **$p < 0.001$, ***$p < 0.0001$.

carotid SMCs, we used commercially available HCtASMCs that we transduced with lentiviral vectors containing the human *HPSE1* gene. The increased HPSE expression (Fig. 4A) was reflected in decreased amounts of HS and/or alterations in HS structures expressed on the cell surface of HPSE-overexpressing cells (hpa), in comparison with ev or wt cells, as shown by decreased staining with anti-HS antibodies (Fig. 4B). The morphology of hpa HCtASMCs also appeared slightly altered in comparison with ev and wt HCtASMCs, with an increased cell surface area (Fig. 4C). To find out whether increased expression of HPSE influences transcription of genes associated with osteogenesis, RNA was isolated from wt-, ev- and hpa HCtASMCs undergoing osteogenic differentiation for 4 and 21 days, respectively. We focused on *RUNX2* and also *SPP1*, which encodes osteopontin, previously demonstrated to play dual roles during bone formation and turnover [32–34]. The mRNA levels of *RUNX2* increased in all cell types during the 21d culture period, however there was no significant difference between hpa in comparison to ev HCtASMCs (Fig. 4D). For *SPP1*, the appearance of the graph suggests a downregulation of gene expression at day 4 and then an increase at the later time point, however statistical significance was not reached, and only a trend ($p = 0.0571$) towards increased *SPP1* levels in hpa vs ev HCtASMCs could be seen at day 21 (Fig. 4E).

For further assessment of osteogenic differentiation in the cell cultures, presence of alkaline phosphatase (ALP) was quantified as numbers of cells expressing the active enzyme. Hpa HCtASMCs demonstrated an increased number of ALP^+ cells (mean = 5.9 ± 0.42) in comparison to ev HCtASMCs (mean = 2.31 ± 0.55), already at 4 days of incubation (Fig. 4F). Presence of heparin, with the intention to inhibit HPSE-mediated effects observed in hpa HCtASMCs, had no impact on the number of ALP^+ cells (mean = 4.88 ± 0.67) at this time point. At 21 days, hpa HCtASMCs (mean = 122 ± 6.5) demonstrated a significant increase in ALP^+ cells in comparison to ev HCtASMCs (mean = 63.8 ± 8.9) and wt HCtASMCs (mean = 53.1 ± 12.6). (Fig. 4G). Unexpectedly, the presence of heparin for 21 days caused a further significant increase in relative numbers of ALP^+ cells in all groups in comparison to non-treated counterparts but the numbers of ALP^+ heparin-treated hpa HCtASMCs (mean = 200 ± 5.8) were also increased in comparison to heparin-treated ev HCtASMCs (mean = 98.3 ± 6.2). An additional observation was that the overall cell count of hpa HCtASMCs was generally lower, possibly due to the larger size of these cells but possibly also due to reduced viability.

3.6. Increased mineralization of cultured human carotid SMCs expressing high levels of HPSE

Exposure of HCtASMCs to osteogenic medium induced mineralization as visualized at 21 days of differentiation, by Alizarin Red staining (Fig. 5). Although calcium-containing precipitates were identified in the cultures of wt or ev HCtASMCs, the staining was substantially increased for hpa HCtASMCs. Furthermore, whereas in the control cell cultures the precipitates appeared as clearly defined, extracellular nodules (Fig. 5D–E), the hpa HCtASMCs displayed a diffuse, widespread staining pattern of AZR with precipitates appearing intracellularly as well as extracellularly (Fig. 5F). The markedly increased mineralization was consistently observed in the hpa HCtASMCs, however, the extent of AZR staining varied slightly between repeated experiments and correlated strongly with reduced cell viability, seen as loss of cells among the hpa HCtASMCs. Scanning electron microscopy of wt or ev HCtASMCs revealed occasional nodules, assumed to correspond with the AZR-stained precipitates in parallel culture wells (Fig. 5G–H). In contrast the hpa HCtASMCs demonstrated widespread fibro-calcific structures along cell membranes, in addition to the extracellular precipitates (Fig. 5I). As shown by high magnification, the structures showed little resemblance with crystals previously described in calcifiying SMCs [35], and had rather a globular appearance (Fig. 5J-L).

4. Discussion

In the present study, we investigated the expression and function of HPSE in vascular calcification associated with atherosclerosis. Gene expression data extracted from the BiKE biobank of human carotid endarterectomies showed that HPSE expression levels primarily correlated with genes associated with differentiation and activity of osteoclasts rather than with osteogenesis. In addition, HPSE protein colocalized with multinucleated, TRAP-positive osteoclast-like cells in carotid plaques. In order to assess the effects of increased HPSE expression on calcification and osteolysis in simplified *in vitro* systems without potential confounding effects mediated by other cell types present in the plaque, we analysed the ability of smooth muscle cells and macrophages/osteoclasts to form and degrade bone respectively. An association between HPSE and osteolysis was corroborated *in vitro,* as an increased osteolytic activity was observed in mouse bone marrow-derived osteoclasts overexpressing human HPSE, in comparison to those from wild-type mice. In contrast, HPSE-overexpressing human carotid SMCs in culture demonstrated an elevated number of alkaline phosphatase-expressing cells and also increased mineralization after osteogenic differentiation.

A possible explanation for the somewhat contradictory findings observed in the clinical atherosclerotic tissue samples in comparison to the *in vitro* osteogenic differentiation of vascular SMCs and also the observations in the *hpa*-tg mouse, is the absence of inflammatory infiltrates in the two latter. Although bone marrow-derived osteoclasts from *hpa*-tg mice displayed an increased osteolytic activity compared to that of wt counterparts, the previously reported increased bone density in these animals [20] suggests that the function of HPSE in this setting is coupled to augmented osteogenesis rather than to osteolysis. In the atherosclerotic plaque on the other hand, HPSE is strongly associated with inflammatory cells as we have previously shown [19], and plaque-infiltrating macrophages are likely the origin of multinucleated osteoclast-like cells in this tissue. Based on our qualitative evaluation of immunohistochemical stainings, large, TRAP-positive osteoclast-like cells containing high numbers of nuclei, generally tended to express CD68 while being devoid of CD163. For smaller-sized cells with fewer nuclei, this dichotomy was less evident. Previous studies demonstrated the expression of CD68 by osteoclast-like cells associated with calcified atherosclerotic vessels, while CD163 was not investigated [36–38]. The question whether osteoclast-like cells are predominantly formed by CD68-positive macrophages and/or whether this has implications for the functional properties of large osteoclast-like cells in atherosclerosis, remains to be fully clarified.

Heparin can act as an inhibitor of HPSE activity by competing with its endogenous substrate, HS [39]. However, depending on the concentration and context it may theoretically also enhance HS-dependent functions [40–42]. The heparin concentration used in the present study was chosen based on initial pilot studies, where higher levels had a clear negative impact on cell viability, above all in the HPSE-overexpressing cells. Our intention was to utilize heparin to inhibit HPSE, in order to reverse potential effects of the enzyme on calcification. Obviously, the added heparin was insufficient as a HPSE inhibitor; on the contrary, it may have functioned as a co-receptor for BMPs and promoted their activity, a similar function previously demonstrated in FGF activity [43]. The indistinguishable effect of heparin on all three subgroups of HCtASMCs also supports a stimulating effect of heparin in osteogenic differentiation, which is more pronounced when HPSE levels are elevated.

It is debated whether calcification contributes to plaque instability or instead exerts a stabilizing function on the affected blood vessel. Osteolysis mediated by osteoclasts derived from inflammatory macrophages represents one possible mechanism for plaque destabilization by degradation of stabilizing homogenous calcified structures within the vessel wall. In the present study, we demonstrate an up-regulation of osteoclast-related markers (TRAP and OSCAR) in carotid plaques from

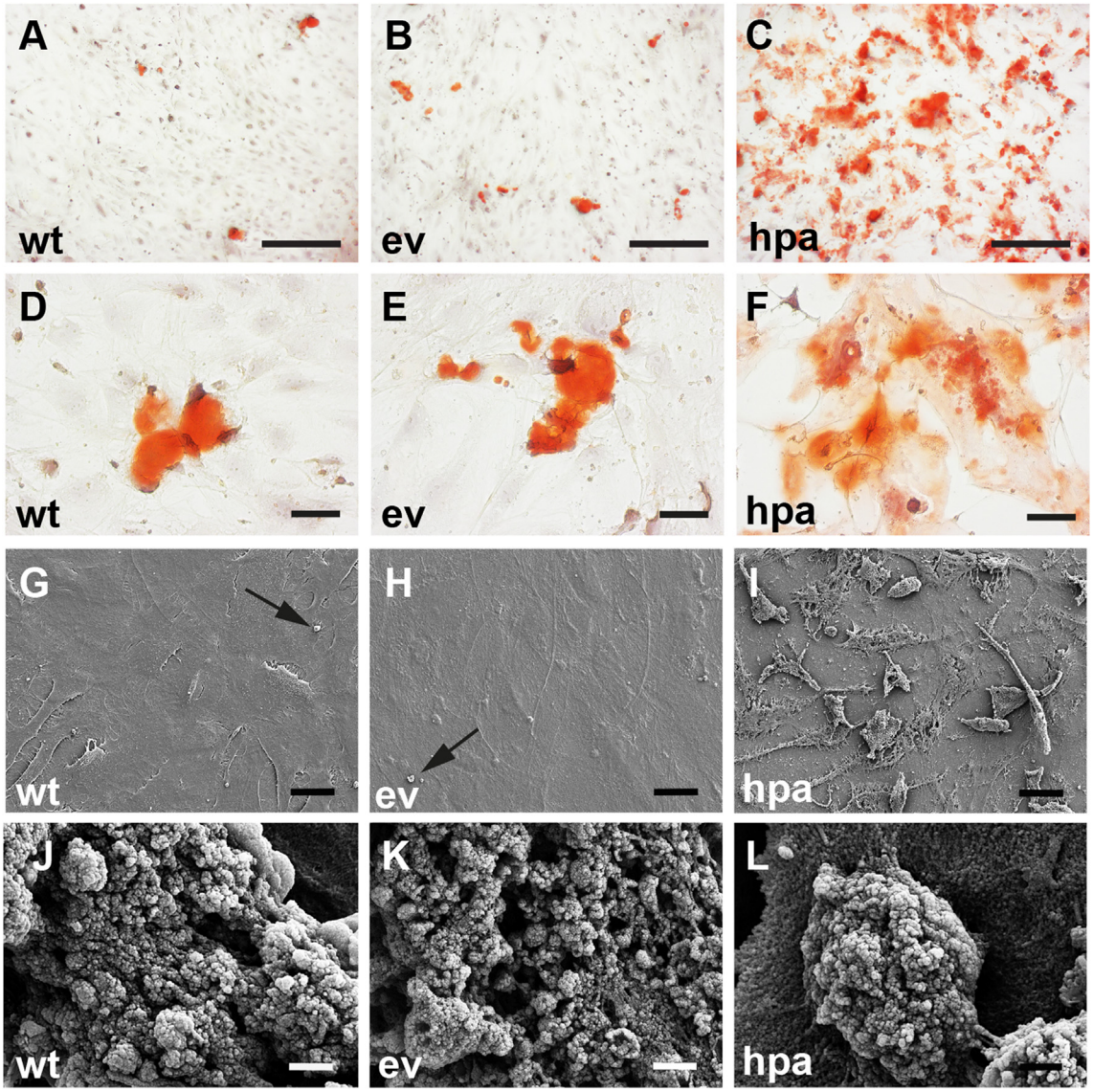

Fig. 5. Increased mineralization of human carotid SMCs overexpressing HPSE.
Brightfield images showing Alizarin Red staining of wt, ev and hpa HCtASMCs exposed to osteogenic differentiation medium for 21 days. Images (A–C) show representative overview images of the cultured cells (size bars represent 200 μm) and (D–F) show representative close-up images of calcified structures (size bars represent 20 μm). Each cell type was assessed in triplicate (n = 3) for each condition and experiments were repeated 3 times. Representative scanning electron microscopy (SEM) images show glutaraldehyde-fixed wt, ev and hpa HCtASMCs after 21 days of exposure to osteogenic differentiation medium. Arrows indicate sparsely occurring calcified nodules in the cultures of wt and ev cells. Size bars in images (G–I) represent 30 μm and bars in images (J–L) represent 100 nm. Each cell type was plated in triplicate (n = 3) for each condition and experiments were repeated twice.

symptomatic patients, which could indicate a link between osteolysis and plaque instability. Moreover, if increased osteolytic activity of osteoclasts, due to high expression levels of HPSE, can be extrapolated to atherosclerotic plaque tissue, this may suggest an indirect role for HPSE in plaque destabilization.

In conjunction with increased mineralization of hpa HCtASMCs, a reduced cell number was evident, indicating a negative effect of calcium precipitation on the viability of these cells. This particular feature of the Hpa HCtASMCs in comparison to control cells was also observed after exposure to high concentrations of inorganic phosphate (unpublished data). An earlier study by Ewence *et al* described vascular smooth muscle cell death as a consequence of induced calcium crystal formation and, in particular, crystals of reduced size [35]. In the present study, the observations from AZR staining after osteogenic differentiation of HCtASMC were that, in contrast to the wt and ev cells where the mineralization appeared to take place extracellularly, the hpa cells additionally displayed tiny AZR-positive structures inside the cells. One possible explanation for the increased mineralization of HPSE-overexpressing SMCs when exposed to osteogenic medium and high inorganic phosphate levels, could be that HS glycosaminoglycans of normal length regulate calcium precipitation in general, which is supported by a recent study by Borland et al., where Syndecan-4 was demonstrated to enhance an inhibitory effect of FGF-2 on mineral deposition induced by organic phosphate in bovine VSMCs [44], but also that they prevent formation of small-sized intracellular calcium crystals, potentially by providing a scaffold on which extracellular calcium precipitation can take place. Hence, another plausible effect of inflammation-induced expression and activity of HPSE in atherosclerotic lesions could be smooth muscle cell death due to formation of small-sized calcium crystals, which in turn would be a consequence of reduced HS chain length. Although speculative, this suggests another potential mechanism for HPSE contribution to atherosclerotic plaque instability. In the histological sections of carotid atherosclerotic lesions, AZR staining in subintimal regions coincided to a large extent with

absence of SMCs, suggesting an association between mineralization and cell death, which is also a previously described phenomenon [45,46]. However, the fact that HPSE staining was weak or absent in these structures and the surrounding cells naturally raises the question to which extent HPSE levels would contribute *in vivo* to increased SMC calcification and death by the above-suggested mechanism.

To our knowledge, this is the first exploration of HPSE in the context of vascular calcification. We combined information from a large biobank representing human atherosclerotic disease, with that obtained from *in vitro* studies, in which simplified cell systems with altered HPSE expression levels were utilized. For a balanced interpretation of the obtained data, several limitations of the study should be taken into consideration. The BiKE biobank is restricted to human endarterectomy specimens and transcriptomic data from advanced, end-stage atherosclerosis (AHA class V-VI), which excludes analyses of HPSE in early disease progression. Additionally, the protocol used for mRNA isolation from BiKE samples does not account for plaque heterogeneity and the corresponding specimen parts used for validation by IHC may contain regions displaying different plaque features. Furthermore, the HPSE levels expressed by the lentivirus-transduced HCtASMCs can be regarded as supra-physiological, with one potential effect being HSPGs with dramatically reduced GAG chain length. It is therefore uncertain to which extent the *in vitro* experiments reflect the processes taking place in the clinical setting where these alterations are presumably more modest in comparison. Lastly, although the commercially available osteogeneic differentiation medium produced a significant and reproducible calcification of HCtASMCs, care should be taken when comparing effects and potential mechanisms with those mediated by clearly defined inducers, such as inorganic or organic phosphate of known concentrations.

In summary, we suggest that the functions of HPSE in vascular calcification may be different depending on the context of the environment. Whereas HPSE plausibly contributes to mineralization and osteogenic differentiation of SMCs and other mesenchymal cells in the absence of inflammation, in the advanced atherosclerotic plaque HPSE may primarily be associated with osteolysis mediated by macrophage-derived osteoclasts.

Conflicts of interest

The authors declared they do not have anything to disclose regarding conflict of interest with respect to this manuscript.

Financial support

This study was supported by funding from The Swedish Heart and Lung Foundation: 20140131 (JPL), 20170584 (UH), the Swedish Research Council: 2015-02595 (JPL), 2017-01070, (UH), 2013-03590 (KHG), The Swedish Cancer Foundation: CAN2015/496 (JPL) and the Åke Wiberg Foundation M15-0222 (SA).

Author contributions

SA, LE and CO conceived and designed the experiments. SA, LE, CO, MLe, MK, MLö conducted the experiments. SA, LE, MK, LPM, LF and CO analysed the data. KHG, SA, LM, JPL and UH contributed with crucial reagents and financial support. SA, LE, JPL, LF, UH and CO wrote the manuscript. All authors read and approved the final manuscript version.

Acknowledgments

We are grateful to Dr. Neta Ilan and Dr. Israel Vlodavsky for providing the lentiviral transfer plasmid and mice and to Dr. Kjell Hultenby for SEM analyses.

Appendix A. Supplementary data

Supplementary data to this article can be found online at https://doi.org/10.1016/j.atherosclerosis.2018.12.027.

References

[1] E. Aikawa, M. Nahrendorf, J.L. Figueiredo, F.K. Swirski, T. Shtatland, R.H. Kohler, F.A. Jaffer, M. Aikawa, R. Weissleder, Osteogenesis associates with inflammation in early-stage atherosclerosis evaluated by molecular imaging in vivo, Circulation 116 (2007) 2841–2850.
[2] T. Nakahara, M.R. Dweck, N. Narula, D. Pisapia, J. Narula, H.W. Strauss, Coronary artery calcification: from mechanism to molecular imaging, JACC Cardiovasc. Imag. 10 (2017) 582–593.
[3] R.M. Kwee, Systematic review on the association between calcification in carotid plaques and clinical ischemic symptoms, J. Vasc. Surg. 51 (2010) 1015–1025.
[4] L. Perisic, S. Aldi, Y. Sun, L. Folkersen, A. Razuvaev, J. Roy, M. Lengquist, S. Akesson, C.E. Wheelock, L. Maegdefessel, A. Gabrielsen, J. Odeberg, G.K. Hansson, G. Paulsson-Berne, U. Hedin, Gene expression signatures, pathways and networks in carotid atherosclerosis, J. Intern. Med. 279 (2016) 293–308.
[5] S.A. Steitz, M.Y. Speer, G. Curinga, H.Y. Yang, P. Haynes, R. Aebersold, T. Schinke, G. Karsenty, C.M. Giachelli, Smooth muscle cell phenotypic transition associated with calcification: upregulation of cbfa1 and downregulation of smooth muscle lineage markers, Circ. Res. 89 (2001) 1147–1154.
[6] Y.V. Bobryshev, Transdifferentiation of smooth muscle cells into chondrocytes in atherosclerotic arteries in situ: implications for diffuse intimal calcification, J. Pathol. 205 (2005) 641–650.
[7] T.M. Doherty, K. Asotra, L.A. Fitzpatrick, J.H. Qiao, D.J. Wilkin, R.C. Detrano, C.R. Dunstan, P.K. Shah, T.B. Rajavashisth, Calcification in atherosclerosis: bone biology and chronic inflammation at the arterial crossroads, Proc. Natl. Acad. Sci. U. S. A. 100 (2003) 11201–11206.
[8] J.R. Bishop, M. Schuksz, J.D. Esko, Heparan sulphate proteoglycans fine-tune mammalian physiology, Nature 446 (2007) 1030–1037.
[9] J. Kreuger, D. Spillmann, J.P. Li, U. Lindahl, Interactions between heparan sulfate and proteins: the concept of specificity, J. Cell Biol. 174 (2006) 323–327.
[10] J.P. Li, M. Kusche-Gullberg, Heparan sulfate: biosynthesis, structure, and function, Int. Rev. Cell Mol. Biol. 325 (2016) 215–273.
[11] A. Molteni, D. Modrowski, M. Hott, P.J. Marie, Alterations of matrix- and cell-associated proteoglycans inhibit osteogenesis and growth response to fibroblast growth factor-2 in cultured rat mandibular condyle and calvaria, Cell Tissue Res. 295 (1999) 523–536.
[12] W.J. Kuo, M.A. Digman, A.D. Lander, Heparan sulfate acts as a bone morphogenetic protein coreceptor by facilitating ligand-induced receptor hetero-oligomerization, Mol. Biol. Cell 21 (2010) 4028–4041.
[13] L. Ling, C. Dombrowski, K.M. Foong, L.M. Haupt, G.S. Stein, V. Nurcombe, A.J. van Wijnen, S.M. Cool, Synergism between wnt3a and heparin enhances osteogenesis via a phosphoinositide 3-kinase/akt/runx2 pathway, J. Biol. Chem. 285 (2010) 26233–26244.
[14] S.M. Cool, V. Nurcombe, The osteoblast-heparan sulfate axis: control of the bone cell lineage, Int. J. Biochem. Cell Biol. 37 (2005) 1739–1745.
[15] I. Vlodavsky, Y. Friedmann, M. Elkin, H. Aingorn, R. Atzmon, R. Ishai-Michaeli, M. Bitan, O. Pappo, T. Peretz, I. Michal, L. Spector, I. Pecker, Mammalian heparanase: gene cloning, expression and function in tumor progression and metastasis, Nat. Med. 5 (1999) 793–802.
[16] N. Ilan, M. Elkin, I. Vlodavsky, Regulation, function and clinical significance of heparanase in cancer metastasis and angiogenesis, Int. J. Biochem. Cell Biol. 38 (2006) 2018–2039.
[17] I. Vlodavsky, P. Beckhove, I. Lerner, C. Pisano, A. Meirovitz, N. Ilan, M. Elkin, Significance of heparanase in cancer and inflammation, Canc. Microenviron.: Offic. J. Int. Canc. Microenviron. Soc. 5 (2012) 115–132.
[18] I. Vlodavsky, M. Blich, J.P. Li, R.D. Sanderson, N. Ilan, Involvement of heparanase in atherosclerosis and other vessel wall pathologies, Matrix Biol.: J. Int. Soc. Matrix Biol. 32 (2013) 241–251.
[19] C. Osterholm, L. Folkersen, M. Lengquist, F. Ponten, T. Renne, J. Li, U. Hedin, Increased expression of heparanase in symptomatic carotid atherosclerosis, Atherosclerosis 226 (2013) 67–73.
[20] V. Kram, E. Zcharia, O. Yacoby-Zeevi, S. Metzger, T. Chajek-Shaul, Y. Gabet, R. Muller, I. Vlodavsky, I. Bab, Heparanase is expressed in osteoblastic cells and stimulates bone formation and bone mass, J. Cell. Physiol. 207 (2006) 784–792.
[21] E. Zcharia, S. Metzger, T. Chajek-Shaul, H. Aingorn, M. Elkin, Y. Friedmann, T. Weinstein, J.P. Li, U. Lindahl, I. Vlodavsky, Transgenic expression of mammalian heparanase uncovers physiological functions of heparan sulfate in tissue morphogenesis, vascularization, and feeding behavior, FASEB J.: Offic. Publ. Fed. Am. Soc. Exp. Biol. 18 (2004) 252–263.
[22] K.J. Manton, D.F. Leong, S.M. Cool, V. Nurcombe, Disruption of heparan and chondroitin sulfate signaling enhances mesenchymal stem cell-derived osteogenic differentiation via bone morphogenetic protein signaling pathways, Stem Cell. 25 (2007) 2845–2854.
[23] Y. Yang, Y. Ren, V.C. Ramani, L. Nan, L.J. Suva, R.D. Sanderson, Heparanase enhances local and systemic osteolysis in multiple myeloma by upregulating the expression and secretion of rankl, Cancer Res. 70 (2010) 8329–8338.
[24] J. Ruan, T.N. Trotter, L. Nan, R. Luo, A. Javed, R.D. Sanderson, L.J. Suva, Y. Yang, Heparanase inhibits osteoblastogenesis and shifts bone marrow progenitor cell fate in myeloma bone disease, Bone 57 (2013) 10–17.

[25] L. Folkersen, D. Diez, C.E. Wheelock, J.Z. Haeggstrom, S. Goto, P. Eriksson, A. Gabrielsen, Generegionscan: A bioconductor package for probe-level analysis of specific, small regions of the genome, Bioinformatics 25 (2009) 1978–1979.
[26] S. Aldi, P.A. Robador, K. Tomita, A. Di Lorenzo, R. Levi, Ige receptor-mediated mast-cell renin release, Am. J. Pathol. 184 (2014) 376–381.
[27] P. Ducy, R. Zhang, V. Geoffroy, A.L. Ridall, G. Karsenty, Osf2/cbfa1: a transcriptional activator of osteoblast differentiation, Cell 89 (1997) 747–754.
[28] G.P. Fadini, M. Albiero, L. Menegazzo, E. Boscaro, S. Vigili de Kreutzenberg, C. Agostini, A. Cabrelle, G. Binotto, M. Rattazzi, E. Bertacco, R. Bertorelle, L. Biasini, M. Mion, M. Plebani, G. Ceolotto, A. Angelini, C. Castellani, M. Menegolo, F. Grego, S. Dimmeler, F. Seeger, A. Zeiher, A. Tiengo, A. Avogaro, Widespread increase in myeloid calcifying cells contributes to ectopic vascular calcification in type 2 diabetes, Circ. Res. 108 (2011) 1112–1121.
[29] S.E. New, E. Aikawa, Role of extracellular vesicles in de novo mineralization: an additional novel mechanism of cardiovascular calcification, Arterioscler. Thromb. Vasc. Biol. 33 (2013) 1753–1758.
[30] M.Y. Speer, H.Y. Yang, T. Brabb, E. Leaf, A. Look, W.L. Lin, A. Frutkin, D. Dichek, C.M. Giachelli, Smooth muscle cells give rise to osteochondrogenic precursors and chondrocytes in calcifying arteries, Circ. Res. 104 (2009) 733–741.
[31] V. Naik, E.M. Leaf, J.H. Hu, H.Y. Yang, N.B. Nguyen, C.M. Giachelli, M.Y. Speer, Sources of cells that contribute to atherosclerotic intimal calcification: an in vivo genetic fate mapping study, Cardiovasc. Res. 94 (2012) 545–554.
[32] H. Shiraga, W. Min, W.J. VanDusen, M.D. Clayman, D. Miner, C.H. Terrell, J.R. Sherbotie, J.W. Foreman, C. Przysiecki, E.G. Neilson, et al., Inhibition of calcium oxalate crystal growth in vitro by uropontin: another member of the aspartic acid-rich protein superfamily, Proc. Natl. Acad. Sci. U. S. A 89 (1992) 426–430.
[33] A.L. Boskey, L. Spevak, E. Paschalis, S.B. Doty, M.D. McKee, Osteopontin deficiency increases mineral content and mineral crystallinity in mouse bone, Calcif. Tissue Int. 71 (2002) 145–154.
[34] A. Franzen, K. Hultenby, F.P. Reinholt, P. Onnerfjord, D. Heinegard, Altered osteoclast development and function in osteopontin deficient mice, J. Orthop. Res.:Offic. Publ. Orthop. Res. Soc. 26 (2008) 721–728.
[35] A.E. Ewence, M. Bootman, H.L. Roderick, J.N. Skepper, G. McCarthy, M. Epple, M. Neumann, C.M. Shanahan, D. Proudfoot, Calcium phosphate crystals induce cell death in human vascular smooth muscle cells: a potential mechanism in atherosclerotic plaque destabilization, Circ. Res. 103 (2008) e28–34.
[36] J.H. Qiao, V. Mishra, M.C. Fishbein, S.K. Sinha, T.B. Rajavashisth, Multinucleated giant cells in atherosclerotic plaques of human carotid arteries: identification of osteoclast-like cells and their specific proteins in artery wall, Exp. Mol. Pathol. 99 (2015) 654–662.
[37] G. Chinetti-Gbaguidi, M. Daoudi, M. Rosa, M. Vinod, L. Louvet, C. Copin, M. Fanchon, J. Vanhoutte, B. Derudas, L. Belloy, S. Haulon, C. Zawadzki, S. Susen, Z.A. Massy, J. Eeckhoute, B. Staels, Human alternative macrophages populate calcified areas of atherosclerotic lesions and display impaired rankl-induced osteoclastic bone resorption activity, Circ. Res. 121 (2017) 19–30.
[38] M. Jeziorska, C. McCollum, D.E. Wooley, Observations on bone formation and remodelling in advanced atherosclerotic lesions of human carotid arteries, Virchows Arch. 433 (1998) 559–565.
[39] I. Vlodavsky, N. Ilan, A. Naggi, B. Casu, Heparanase: structure, biological functions, and inhibition by heparin-derived mimetics of heparan sulfate, Curr. Pharmaceut. Des. 13 (2007) 2057–2073.
[40] H.J. Hausser, R.E. Brenner, Low doses and high doses of heparin have different effects on osteoblast-like saos-2 cells in vitro, J. Cell. Biochem. 91 (2004) 1062–1073.
[41] G. Chatzinikolaou, D. Nikitovic, A. Asimakopoulou, A. Tsatsakis, N.K. Karamanos, G.N. Tzanakakis, Heparin–a unique stimulator of human colon cancer cells' growth, IUBMB Life 60 (2008) 333–340.
[42] J. Jia, M. Maccarana, X. Zhang, M. Bespalov, U. Lindahl, J.P. Li, Lack of l-iduronic acid in heparan sulfate affects interaction with growth factors and cell signaling, J. Biol. Chem. 284 (2009) 15942–15950.
[43] N. Jastrebova, M. Vanwildemeersch, A.C. Rapraeger, G. Gimenez-Gallego, U. Lindahl, D. Spillmann, Heparan sulfate-related oligosaccharides in ternary complex formation with fibroblast growth factors 1 and 2 and their receptors, J. Biol. Chem. 281 (2006) 26884–26892.
[44] S.J. Borland, T.G. Morris, S.C. Borland, M.R. Morgan, S.E. Francis, C.L.R. Merry, A.E. Canfield, Regulation of vascular smooth muscle cell calcification by syndecan-4/fgf-2/pkcalpha signalling and cross-talk with tgfbeta, Cardiovasc. Res. 113 (2017) 1639–1652.
[45] J.L. Reynolds, A.J. Joannides, J.N. Skepper, R. McNair, L.J. Schurgers, D. Proudfoot, W. Jahnen-Dechent, P.L. Weissberg, C.M. Shanahan, Human vascular smooth muscle cells undergo vesicle-mediated calcification in response to changes in extracellular calcium and phosphate concentrations: a potential mechanism for accelerated vascular calcification in esrd, J. Am. Soc. Nephrol.:JASN 15 (2004) 2857–2867.
[46] R.C. Shroff, R. McNair, J.N. Skepper, N. Figg, L.J. Schurgers, J. Deanfield, L. Rees, C.M. Shanahan, Chronic mineral dysregulation promotes vascular smooth muscle cell adaptation and extracellular matrix calcification, J. Am. Soc. Nephrol.:JASN 21 (2010) 103–112.